Journal of Process Control 21 (2011) 1361–1369

Contents lists available at ScienceDirect

Journal of Process Control

journal homepage: www.elsevier.com/locate/jprocont

Optimal control of convection–diffusion process with time-varying spatial domain: Czochralski crystal growth

James Ng, Stevan Dubljevic*

Department of Chemical & Materials Engineering, University of Alberta, Canada T6G 2V4

ARTICLE INFO

Article history:
Received 4 December 2010
Received in revised form 29 July 2011
Accepted 30 July 2011
Available online 7 September 2011

Keywords:
Parabolic partial differential equation
Distributed parameter system
Optimal control
Czochralski crystal growth process

ABSTRACT

This paper considers the optimal control of convection–diffusion systems modeled by parabolic partial differential equations (PDEs) with time-dependent spatial domains for application to the crystal temperature regulation problem in the Czochralski (CZ) crystal growth process. The parabolic PDE model describing the temperature dynamics in the crystal region arising from the first principles continuum mechanics is defined on the time-varying spatial domain. The dynamics of the domain boundary evolution, which is determined by the mechanical subsystem pulling the crystal from the melt, are described by an ordinary differential equation for rigid body mechanics and unidirectionally coupled to the convection–diffusion process described by the PDE system. The representation of the PDE as an evolution system on an appropriate infinite-dimensional space is developed and the analytic expression and properties of the associated two-parameter semigroup generated by the nonautonomous operator are provided. The LQR control synthesis in terms of the two-parameter semigroup is considered. The optimal control problem setup for the PDE coupled with the finite-dimensional subsystem is presented and numerical results demonstrate the regulation of the two-dimensional crystal temperature distribution in the time-varying spatial domain.

1. Introduction

A large number of industrial systems exhibit time-varying features in which certain parameters of the system change over the course of the process. The methods employed in the formation and treatment of materials may result in, for example, chemical reactions, phase transitions, deformations or a combination of these behaviours, and therefore introduce complexities in model-based controller design. The Czochralski (CZ) crystal growth process, utilized for the production of semiconductor materials for the microelectronics industry, is a prime example in which a time-dependent feature of the system is the change in material domain and is the motivating example behind our study.

In the CZ crystal growth process, large boules of single crystals, typically Si, GaAs, InP, and CdTe, are formed in a thermal environment, whereby a crystal seed is slowly drawn from a pool of melt by a mechanical pulling arm. The material growth by solidification at the crystal–melt interface is affected by variations in the thermal fields of the ambient and melt temperatures, as well as the rate of pulling. These conditions are significant factors which contribute to the overall product quality where the objective of the batch processing strategy is to yield high-purity, defect and dislocation free crystals with constant diameter. The latter specification is vulnerable to fluctuations in heat transfer caused by turbulent convection in the melt environment, and also to longer term disturbances in the ambient temperature and changes in the melt level.

The complexity in modelling the dynamics of the CZ crystal growth process is reflected in the numerous works dedicated to the analyses of the multi-physics system which include studies of the transport phenomena associated with the crystal temperature, crystal–melt interface, melt dynamics, and crystal pull rate (see [6–9]). A more complete survey of the modelling and dynamical analyses of the process is contained in the review articles by Brown [6] and Lan [16], which also describe the usage and challenges in the design and implementation of active control methodologies for single crystal growth. For example, the maintenance of the crystal shape is a subject of considerable interest. Several controlled growth methods are based on models which incorporate the relationships between the crystal, ambient and melt temperatures, and have led to proposed strategies in which diameter control is achieved via combinations of crucible heater, bottom heater and crystal pull rate actuation (see [7–9]).

Another important control problem which has garnered less attention is the regulation of the crystal temperature distribution during the process which is important in counteracting the

* Corresponding author. Tel.: +1 780 248 1596; fax: +1 780 292 2881
E-mail addresses: jcng@ualberta.ca (J. Ng), stevan.dubljevic@ualberta.ca (S. Dubljevic).

0959-1524/$ – see front matter.
doi:10.1016/j.jprocont.2011.07.017

fluctuations in the rate at which the crystal cools which can cause large thermoelastic stresses leading to micro-defect and dislocation generation within the grown crystal [23,25]. Therefore, the complex transport phenomena models of the crystal temperature dynamics are developed by utilizing mass and energy balance relations which yield parabolic partial differential equations (PDEs) defined on time-varying spatial domains [9]. In the process control field there are several works which consider various model representations and control strategies for parabolic PDEs with time-varying spatial domains along with different control objectives which include the temperature stabilization problem using robust control methods [3], the boundary stabilization by manipulation of the temperature field [13], and the inverse Stefan problem in which the boundary evolution is known *a priori* [11]. Another approach considers the optimal stabilization of the temperature distribution of a material, for example in annealing type processes, by varying the spatial domain in which the domain motion is described by a finite-dimensional mechanical subsystem (see [26,27]).

Motivated by the process complexity and the lack of optimal control realization for the CZ crystal growth process, in this work we provide a model development for the parabolic PDE on the time-varying spatial domain, and consider the optimal control formulation for the CZ crystal temperature regulation problem. As previously mentioned, it is of interest to control the rate at which the crystal cools in order to prevent material defects and dislocation generation and it is also of interest to stabilize the rate of pulling around some desired value. Therefore, the optimal regulation of the temperature distribution in the time-varying spatial domain around a pre-specified nominal distribution is required. The system is characterized by the unidirectional coupling of the domain motion, which is determined by the mechanical pulling which draws the crystal from the melt with dynamics described by a second order ODE, to the parabolic PDE system which describes the transient temperature distribution in the grown crystal. The controller synthesis for the crystal temperature regulation problem is considered from the perspective of infinite-dimensional systems theory whereby the PDE is represented as an evolutionary equation on an appropriately defined function space with nonautonomous operator which generates a two-parameter semigroup. In this form, the control problem is considered using linear-quadratic optimal control theory for nonautonomous infinite-dimensional systems. To address the issue of practical realization, the finite-dimensional system representation of the PDE system is obtained, and we consider the simultaneous control problem of the crystal temperature regulation and the stabilization of the domain motion around a nominal steady state value. A low order controller for the crystal temperature regulation problem is proposed and numerical results are provided including the comparison of the optimal controller to conventional proportional controllers.

This paper is organized as follows: in Section 2 the boundary evolution due to the mechanical pulling arm is described in terms of a second order ODE and the crystal temperature dynamics are described by a parabolic PDE defined on the time-varying spatial domain. In Section 3, the PDE is represented as an abstract evolution equation on an infinite-dimensional space with nonautonomous parabolic operator which generates a two-parameter semigroup. This representation enables the use of time-varying infinite-dimensional systems theory to pose the time-varying optimal control problem in Section 4. In Section 5, the finite-dimensional system representation of the PDE is determined and augmented with the mechanical pulling arm subsystem, to facilitate the numerical implementation of the control problem for the temperature regulation and domain motion. The optimal control synthesis of the augmented system is presented and numerical results are provided in Section 6. Finally, Section 7 concludes the paper with a summary of results.

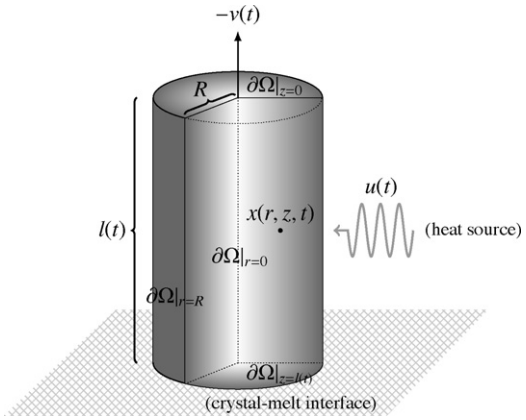

Fig. 1. Cutaway of general process diagram of axisymmetric cylindrical slab with radius R, length $l(t)$, and temperature distribution $x(r, z, t)$ for $(r, z) \in \Omega$ at time $t \in [0, T]$. The spatial domain time-dependence is due to the change in the boundary at $\partial\Omega|_{z=l(t)}$ which is moving with velocity $v(t)$. The temperature distribution of the slab is regulated by heat input $u(t)$ applied to the boundary at $\partial\Omega|_{r=1}$.

2. Model description

The crystal region is considered as an axisymmetric and time-varying spatial domain with unit radius $R = 1$ and length $l(t)$. The spatial domain motion is due to the crystal pull rate $v(t)$ which determines the growth in the crystal at the boundary $z = l(t)$, where $l(t) > 0$ is the crystal length, see Fig. 1. The boundary evolution is determined by a mechanical actuator pulling the crystal from the melt. In practice the crystal pull rate is slow, and we approximate the dynamics of the mechanical subsystem around some nominal pull rate by the second order ordinary differential equation (ODE) for rigid body mechanics:

$$m_s \frac{d^2\tilde{l}}{dt^2} + a_d \frac{d\tilde{l}}{dt} + b_e \tilde{l} = f_{\text{mec}} \tag{1}$$

where m_s, a_d and b_e are finite and represent constant mass, damping, and elastic coefficients of the rigid body system, f_{mec} is the force applied by the actuator, and $\tilde{l}(t)$ is the deviation form of $l(t)$. The function $x : \Omega \times [0, T] \to \mathbb{R}$ represents the temperature of the time dependent spatial domain, denoted $\Omega := \{(r, z) : 0 < r < 1, 0 < z < l(t)\}$ at some time $t \in [0, T]$, around the desired nominal distribution in dimensionless form with dynamics described by the parabolic PDE model:

$$\begin{aligned} \text{Pe}\frac{\partial x}{\partial t} &= \nabla \cdot \kappa_s \nabla x - \text{Pe}\, v(t)\frac{\partial x}{\partial z} \quad \text{in} \quad \Omega \times (0, T] \\ x(r, z, 0) &= x_0(r, z) \qquad\qquad \text{in} \quad \Omega \end{aligned} \tag{2}$$

where $x_0(r, z)$ is the initial condition. The Peclet number $\text{Pe} = v_0 R_c C_p \rho_c > 0$ is the dimensionless variable with constants v_0, R_c, and C_p denoting the nominal pull rate, scaled crucible radius and crystal specific heat capacity, respectively. It is assumed that as the crystal is pulled from the melt, solidification at the solid–melt interface results in a crystal structure of constant density ρ_c. Eq. (2), which is derived in Appendix A, is similar to the model utilized in [9] and [10] with the exception that the scaled thermal conductivity in these works is a function of the temperature, i.e. $\kappa_s = \kappa_s(x)$. In this work, it is assumed that the thermal effects on κ_s are sufficiently small due to the high crystal purity such that κ_s is homogeneous and constant throughout Ω for all $t \in [0, T]$. One can notice that the PDE in Eq. (2) is characterized by the presence of the boundary velocity term $v(t)$. In particular, the convective transport term $v(t)\partial x/\partial z$ is due to the underlying spatial domain motion which vanishes if

the domain motion becomes isochronic, and is time-invariant if the pull rate is constant.

The crystal temperature at the crystal–melt interface is assume to be equal to the melt temperature, and similarly across the crystal-ambient temperature fields [9]. Then the boundary conditions imposed in Eq. (2) are expressed as:

$$\frac{\partial x}{\partial n}|_{\partial\Omega} = 0, \quad \text{on} \quad \partial\Omega \times (0, T] \tag{3}$$

where n is the unit outward normal to $\partial\Omega$.

Remark 1. In particular, one can impose more general boundary conditions of the Robin type which will not substantially change the results of the subsequent sections except that the eigenfunctions in Eq. (12) with the associated eigenvalues in Eq. (14) will not be analytically expressed.

3. Infinite-dimensional system representation

The optimal control formulation proposed in the subsequent section requires the representation of the PDE in Eq. (2) as an evolution system on some appropriate Banach space. In order to handle the time-dependence of the spatial domain, the following function space description provides a suitable framework such that the representation of the PDE in Eq. (2) can be handled using standard infinite-dimensional systems theory.

3.1. Function space description

Let $\mathcal{X}$ and $\mathcal{Y}$ denote two general Banach spaces and $\mathcal{L}(\mathcal{X}, \mathcal{Y})$ denotes the space of bounded linear operators $\mathcal{T}: \mathcal{X} \to \mathcal{Y}$ and $\mathcal{L}(\mathcal{X}) = \mathcal{L}(\mathcal{X}, \mathcal{X})$. At some time $t \in [0, T]$, the spatial domain $\Omega \subset \mathbb{R}^2$ is a bounded open set with smooth boundary $\partial\Omega$. The largest spatial domain configuration is denoted $\mathbf{\Omega} \subset \mathbf{R}^2$ where for all $t \in I_j$, $I_j \subset [0, T]$, there is a sequence of subdomains $\{\Omega_j\} \subset \mathbb{R}^2$ such that $\Omega_{j_1} \subset \Omega_{j_2} \subset \cdots \subset \mathbf{\Omega}$ for each j. The space $L^2(\Omega_j)$ of measurable functions $\phi(r, z, t)$ and $\psi(r, z, t)$ with $\int_\Omega |\phi|^2 d\mu < \infty$ at each time $t \in I_j$, is a Hilbert space with inner product:

$$\langle \phi, \psi \rangle_{L^2(\Omega_j)} = \int_{\Omega_j} \alpha_j \, \phi \, \psi \, dr \, dz \tag{4}$$

where:

$$\alpha_j(t) = \begin{cases} 1, & t \in I_j \\ 0, & t \notin I_j \end{cases} \tag{5}$$

That is, $L^2(\Omega_j)$ forms a family of function spaces for ϕ and ψ defined for each $t \in I_j$ and is generalized as follows. for spatial domain Ω at some time $t \in [0, T]$ the $L^2(\Omega)$ inner product $\langle \cdot, \cdot \rangle$ is given by:

$$\langle \phi, \psi \rangle = \int_\Omega \alpha(t) \phi(r, z, t) \psi(r, z, t) dr dz \tag{6}$$

3.2. Nonautonomous evolution system representation

The PDE in Eq. (2) is expressed as:

$$\frac{\partial x}{\partial t} = \mathcal{A}(r, z, t)x \tag{7}$$

with the boundary conditions in Eq. (3). In cylindrical coordinates, the operator $\mathcal{A}(r, z, t)$ is defined as:

$$\mathcal{A}(r, z, t)x := \frac{1}{r}\frac{\partial}{\partial r}\left(\kappa_0 r \frac{\partial x}{\partial r}\right) + \kappa_0 \frac{\partial^2 x}{\partial z^2} - v(t)\frac{\partial x}{\partial z} \tag{8}$$

for $\kappa_0 = \kappa_s/\text{Pe}$. The expression of the PDE in Eq. (7) as an abstract evolution system requires the establishment of the following properties. For each $t \in [0, T]$, the coefficients of the characteristic equation associated with the principle part of the operator $\mathcal{A}(r, z, t)$ satisfy:

$$\kappa_0(\xi^2 + \eta^2) \neq 0, \quad \text{forall} \quad (\xi, \eta) \neq (0, 0) \in \Omega \tag{9}$$

which is equivalent to $\kappa_0^2 > 0$ since κ_s and Pe are each positive. Eq. (9) implies that there are no real characteristics of the operator $\mathcal{A}(r, z, t)$ given in Eq. (8) such that:

E1. The operator $\mathcal{A}(r, z, t)$ is an *elliptic operator* of second order for each $t \in [0, T]$.

The description of the boundary motion with dynamics governed by the second order ODE in Eq. (1) implies that:

E2. The boundary velocity $v(t)$ is a smooth function (sufficiently Hölder continuous) which satisfies:

$$|v(t) - v(s)| \leq L|t - s|^\beta \tag{10}$$

for $s, t \in [0, T]$ and constants $L > 0$ and $\beta \in (0, 1]$.

It is known from Pazy [21] (Chapter 7.6, Lemma 6.1) that the properties E1–E2 are sufficient in the expression of the initial and boundary value problem in Eq. (7) to be posed as an abstract evolution system on the infinite-dimensional function space $L^2(\Omega)$ with solution provided in terms of a two-parameter semigroup. In order to obtain the explicit expression of this two-parameter semigroup, the eigenfunctions and eigenvalues of the operator $\mathcal{A}(r, z, t)$ and the adjoint $\mathcal{A}^*(r, z, t)$ are determined by standard methods (e.g. separation of variables) and application of the appropriate boundary conditions at each $t \in [0, T]$. Therefore, for $0 \leq r \leq 1$, the eigenfunctions are determined as:

$$\phi_m^{(1)}(r) = \frac{\sqrt{2}}{J_0(\alpha_m)} J_0(\alpha_m r) \tag{11}$$

for $m \in \mathbb{N}$, where J_p are Bessel functions of the first kind and pth order, and $\alpha_m = \{0, 3.83, 7.016, 10.173, 13.323, \dots\}$ are the mth zeros of J_1. The functions $\phi_m^{(1)}(r)$ in Eq. (11) are orthonormal to the eigenfunctions $\psi_m^{(1)}(r) := r\phi_m^{(1)}(r)$ of the corresponding adjoint operator. In the same way, for $0 \leq z \leq l(t)$, and each $t \in [0, T]$, the eigenfunctions are determined as:

$$\begin{aligned} \phi_n^{(2)}(z, t) &= A_n e^{\frac{1}{2}\kappa_0^{-1} v(t) z} \left(\cos\left(\frac{n\pi}{l(t)} z\right) - \frac{1}{2}\kappa_0^{-1} \frac{v(t)}{\left(n\pi/l(t)\right)} \sin\left(\frac{n\pi}{l(t)} z\right) \right) \\ A_n(t) &= \sqrt{\frac{2}{l(t)}} \left(1 + \left(\frac{v(t)}{2\kappa_0 \left(n\pi/l(t)\right)} \right)^2 \right)^{-\frac{1}{2}} \end{aligned} \tag{12}$$

for $n \in \mathbb{N}$ and are orthonormal to the adjoint eigenfunctions $\psi_n^{(2)}(z) = \exp(-\kappa_0^{-1} v(t) z)\phi_n^{(2)}(z)$. We remark here that the notations (1) and (2) are utilized only to distinguish arguments of the functions $\phi^{(1)}(r)$ and $\phi^{(2)}(z, t)$. The family of eigenvalues $\{\Lambda_{mn}(t)\}_{t \in [0,T]}$, $m, n = 1, 2, \dots$ of the operator $\mathcal{A}(r, z, t)$ and adjoint $\mathcal{A}^*(r, z, t)$ are:

$$\Lambda_{mn}(t) = \lambda_n(t) - \kappa_0 \alpha_m^2 \tag{13}$$

where,

$$\lambda_n(t) = -\kappa_0 \left(\frac{n\pi}{l(t)}\right)^2 - \frac{1}{2}\kappa_0^{-1}\frac{v(t)^2}{2} \tag{14}$$

which correspond at each $t \in [0, T]$ to the set of eigenfunctions of the operator $\mathcal{A}(r, z, t)$:

$$\phi_{mn}(r, z, t) := \phi_m^{(1)}(r)\phi_n^{(2)}(z, t) \tag{15}$$

and the adjoint $\mathcal{A}^*(r, z, t)$:

$$\psi_{mn}(r, z, t) := \psi_m^{(1)}(r)\psi_n^{(2)}(z, t) \tag{16}$$

For all $t \in [0, T]$, the eigenfunctions in Eqs. (15) and (16) form a family of time-dependent functions $\{\phi_{mn}(t)\}_{t\in[0,T]}$ and $\{\psi_{mn}(t)\}_{t\in[0,T]}$ which form an orthonormal basis of $L^2(\Omega)$, and at each $t \in [0, T]$, correspond to the family of time-dependent functions $\{\Lambda_{mn}(t)\}_{t\in[0,T]}$.

Consider the family of linear operators $\mathcal{A}(t)$, $t \in [0, T]$ which is associated with the operator $\mathcal{A}(r, z, t)$ in Eq. (8). The domain of $\mathcal{A}(t)$ is defined as:

$$D(\mathcal{A}(t)) := \{x \in L^2(\Omega),\ x, x_r, x_z,\ \text{are a.c.},\ x_{rr}, x_{zz} \in L^2(\Omega),$$
$$x_r|_{r=0} = 0, x_r|_{r=1} = 0,\ x_z|_{z=0} = 0,\ x_z|_{z=l(t)} = 0\} \tag{17}$$

where x_r, x_{rr} denote the first and second order partial derivatives with respect to r, respectively (similarly for x_z and x_{zz}), and a.c. means absolutely continuous. Then for $x(t) \in D(\mathcal{A}(t))$, we define:

$$\mathcal{A}(t)x := \mathcal{A}(r, z, t)x \tag{18}$$

The initial and boundary value problem in Eq. (7) is expressed in terms of the nonautonomous evolution system:

$$\frac{dx}{dt} = \mathcal{A}(t)x, \qquad x(0) = x_0 \tag{19}$$

where the operator $\mathcal{A}(t) : D(\mathcal{A}(t)) \subset L^2(\Omega) \to L^2(\Omega)$ in Eq. (17), satisfies the following properties (see [21], Chapter 5.6):

F1. For every $t \in [0, T]$, the resolvent $R(\lambda, \mathcal{A}(t))$ exists for all λ with $\mathrm{Re}\lambda \le 0$ and

$$R(\mathcal{A}(t), \mu) \le \max_{m,n,t\in[0,T]} (\Lambda_{mn}(t) - \mu)^{-1} \tag{20}$$

which gives that $\|R(\mathcal{A}(t), \lambda)\| \le L_1(|\mu| + 1)^{-1}$. Then $\mathcal{A}(t)$ is a sectorial operator of $L^2(\Omega)$ for every $t \in [0, T]$.

F2. Since $\{0\} \ne \sigma(\mathcal{A}(\cdot))$ for all $t \in [0, T]$ the operator $\mathcal{A}(t)$ has a bounded inverse $\mathcal{A}(t)^{-1}$ on $L^2(\Omega)$ such that

$$\|(\mathcal{A}(t) - \mathcal{A}(s))\mathcal{A}(\tau)^{-1}\| \le L_2|t - s|^{\alpha} \tag{21}$$

for $s, t, \tau \in [0, T]$, and constants $L_2 > 0$ and $\alpha \in (0, 1]$.

Then by Pazy [21] (Chapters 5.1 and 5.6, Theorem 6.1) the solution of the nonhomogeneous initial value problem in Eq. (19) is expressed as:

$$x(t) = U(t, s)x_0, \qquad 0 \le s \le t \le T \tag{22}$$

where $U(t, s)$ is a unique two-parameter semigroup with analytic expression provided in the following Theorem 1.

Theorem 1. *The eigenfunctions in Eqs. (15) and (16) form a family of time-dependent functions with members denoted as $\phi_{mn}(t) = \phi_m^{(1)}(r)\phi_n^{(2)}(z, t)$ and $\psi_{mn}(t) = \psi_m^{(1)}(r)\psi_n^{(2)}(z, t)$ and at each $t \in [0, T]$, correspond to the family of time-dependent functions $\{\Lambda(t)\}_{t\in[0,T]}$ with members $\Lambda_{mn}(t) \in C^1([0, T])$. For $D(\mathcal{A}(t))$ given in Eq. (17), consider the operator $\mathcal{A}(t) : D(\mathcal{A}(t)) \to L^2(\Omega)$ defined as:*

$$\mathcal{A}(t) := \sum_{m,n=1}^{\infty} \mathcal{F}_{mn}(t)\langle\,\cdot\,, \psi_{mn}(t)\rangle\phi_{mn}(t)$$
$$\text{with} \tag{23}$$
$$\mathcal{F}_{mn}(t) = \left\{\left[t\frac{d}{dt}\lambda_n(t) + \lambda_n(t) - \kappa_0\alpha_m^2\right]\phi_n^{(2)}(t) + \frac{\partial}{\partial t}\phi_n^{(2)}(t)\right\}\phi_n^{(2)}(t)^{-1}$$

The operator $\mathcal{A}(t) : D(\mathcal{A}(t)) \subset L^2(\Omega) \to L^2(\Omega)$ is the infinitesimal generator of the two-parameter semigroup $U(t, s)$ defined as:

$$U(t, s)x(s) := \sum_{m,n=1}^{\infty} e^{\Lambda_{mn}(t)t - \Lambda_{mn}(s)s}\langle x(s), \psi_{mn}(s)\rangle\phi_{mn}(t) \tag{24}$$

for $0 \le s \le t \le T$ and $x(s) \in L^2(\Omega)$.

To demonstrate that $\mathcal{A}(t)$ is the infinitesimal generator of the two-parameter semigroup $U(t, s)$, one needs to check if the operator $U(t, s)$ satisfies the following: G1.) $U(t, s)$ is bounded; G2.) $U(t, t) = I$, $U(t, s) = U(t, s^*)U(s^*, s)$ for $0 \le s \le s^* \le t \le T$; and G3.) $U(t, s)$ is differentiable for $0 \le s \le t \le T$ with:

$$\frac{\partial U(t, s)}{\partial t} = \mathcal{A}(t)U(t, s) \quad \text{and} \quad \frac{\partial U(t, s)}{\partial s} = -U(t, s)\mathcal{A}(s)$$

which are verified in Appendix B. Satisfaction of these properties allow us to consider the crystal temperature regulation problem in the following section in terms of the two-parameter semigroup.

Remark 2. One can recall that the notion of the energy of a parabolic PDE system is usually described by the eigenvalue spectrum of the operator. A unique transport-phenomena associated with the spectral characteristic of the operator $\mathcal{A}(t)$ is that the contribution of the domain motion is manifested in the eigenvalues $\Lambda_{mn}(t)$ as the addition additional term in Eq. (14) which has the features of the kinetic energy associated with the boundary motion, i.e. $E_k = v(t)^2/2$. The eigenvalues evolve over time as determined by the boundary velocity and the eigenfunctions in Eqs. (15)–(16) depend on both the velocity $v(t)$ and length of the domain, $l(t)$. One also notes that as the boundary motion approaches zero, $v(t) \to 0$ and $l(t) \to l_c$ where l_c is constant, the eigenfunctions $\phi_m(r, z, t)$ and $\psi_n(r, z, t)$ and eigenvalues converge to those of the standard parabolic PDE on a fixed spatial domain.

4. Controller design

In this section, we consider the optimal control problem for the PDE system given by Eq. (2). Although in several works the boundary control problem for nonautonomous systems of parabolic type has been explored within different frameworks (see for example [1,2]), in this work, we consider the approach to the boundary control formulation which is proposed in [22].

4.1. Optimal boundary control formulation

The input $u(t) \in \mathbb{R}$ is applied at $r = 1$ with function $b(z_c) = (1/2\varepsilon_1)\delta_{[z_c-\varepsilon_1, z_c+\varepsilon_1]}(z)$, $\varepsilon_1 > 0$ on some finite interval $[z_c - \varepsilon_1, z_c + \varepsilon_1]$ around the point $z_c \in (0, l(t))$. The boundary control problem is converted to a distributed control problem (inside the domain) by use of the Dirac delta function denoted $\delta(r - 1)$. The input operator $\mathcal{B}(t)$ is the linear and bounded, i.e. $\mathcal{B}(t) \in \mathcal{L}(\mathbb{R}, \mathcal{X})$ where:

$$\mathcal{B}(t)u(t) := \int_{\Omega} b(z_c)\delta(r - 1)\phi_{mn}(r, z, t)u(t)dr\,dz$$
$$= \int_{\Omega} b(z_c)\phi_{mn}(1, z, t)u(t)dr\,dz \tag{25}$$

The output measurement $y(t) = \mathcal{C}(t)x(t)$ is taken at the radial boundary $r = 1$ around the point $z_o \in (0, l(t))$ and it is similarly defined as the function $b(z_c)$. The boundary control problem is then expressed as:

$$\frac{dx}{dt} = \mathcal{A}(t)x + \mathcal{B}(t)u(t)$$
$$y(t) = \mathcal{C}(t)x \tag{26}$$

In this form, we consider the finite-time horizon LQ-optimal state feedback control problem for the system in Eq. (26) which is based on the minimization of the cost functional:

$$J(x, u) = \int_0^T \left(|\mathcal{C}(\tau)x(\tau)|_Q^2 + |u(\tau)|_{\mathcal{R}}^2\right)d\tau + \langle Qx(T), x(T)\rangle \tag{27}$$

for any initial state $x_0 \in \mathcal{X}$ and weight $Q \in \mathcal{L}(\mathcal{X})$. The minimizing input is denoted $u_{\mathrm{opt}}(t) \in L^2([0, T); \mathbb{R})$ and is associated with the

input penalty term $\mathcal{R} \in \mathbb{R}$ and the optimal pair $u_{\text{opt}}(t)$ and $x_{\text{opt}}(t)$ are related by the feedback formula:

$$u_{opt}(t) = -\mathcal{R}^{-1}\mathcal{B}^{*}(t)\Pi(t)x_{opt}(t) \tag{28}$$

The minimizing solution to Eq. (27) is determined by the operator $\Pi(t) \in \mathcal{L}(\mathcal{X})$ which is the unique nonnegative solution of the differential Riccati equation:

$$\dot{\Pi}(t) + \mathcal{A}(t)^{*}\Pi(t) + \Pi(t)\mathcal{A} - \Pi(t)\mathcal{B}(t)\mathcal{R}^{-1}\mathcal{B}^{*}(t)\Pi(t) + \mathcal{C}^{*}(t)\mathcal{C}(t) = 0 \tag{29}$$

with $\Pi(T) = Q$ and where $\dot{\Pi}(t)$ is the derivative of $\Pi(t)$ with respect to time (see [5,20]). The mild form expression of Eq. (29) is given in terms of $U(t, s)$ as:

$$\Pi(t)x = U^{*}(T, t)QU(T, t)x + \int_{t}^{T} U^{*}(\tau, t)U(\tau, t)x d\tau - \int_{t}^{T} U^{*}(\tau, t)\Pi(\tau)\mathcal{B}(\tau)\mathcal{R}^{-1}\mathcal{B}^{*}(t)\Pi(\tau)U(\tau, t)x\, d\tau \tag{30}$$

Solving Eq. (29) yields the optimal input $u^{\min}_{t\in[0,T]}$ and the optimal state trajectory as the mild solution of the state feedback system $dx/dt = (\mathcal{A}(t) - \mathcal{B}(t)\mathcal{R}^{-1}\mathcal{B}^{*}(t)\Pi(t))x(t)\ 0 \le \tau < t \le T, x(0) = x_0$ which is expressed as:

$$x(t) = \sum_{m,n=1}^{\infty} e^{\Lambda_{mn}(t)t}\langle x_0, \psi_{mn}(0)\rangle\phi_{mn}(t) - \int_{0}^{t} U(t, \tau)\sum_{m,n=1}^{\infty}\mathcal{B}(t)\mathcal{R}^{-1}\mathcal{B}^{*}(t)\Pi(t)\langle x(\tau), \psi_{mn}(\tau)\rangle\phi_{mn}(\tau)d\tau \tag{31}$$

The numerical solution for the optimal input u_{opt} can be determined by utilizing the eigenfunctions in Eqs. (15) and (16) which form a orthonormal basis of $L^2(\Omega)$ at each $t \in [0, T]$ in order to reduce Eq. (29) to an infinite dimensional system of quadratic equations which can then be solved. However, implementation to a physical system requires truncation of terms in the optimal control law which is given as an infinite sum. The numerical approach in the following section provides both, the foundation to simulate the closed loop PDE system in Eqs. (2) and (3) and also an appropriate method to compute the optimal stabilizing input based on the finite-dimensional differential matrix Riccati equation.

5. Numerical implementation

This section provides an overview of the numerical approach utilized to simulate the closed loop PDE system in Eqs. (2) and (3). A more thorough treatment of the Galerkin method pertaining to the variational form of the problem and existence and uniqueness of solutions is omitted (see for example [12,19,14]).

5.1. Galerkin approximation

In this section, we invoke the Galerkin method in order to approximate the infinite-dimensional system representation of the PDE as a finite-dimensional problem by projection of the PDE onto a finite-dimensional space X utilizing the complete set of eigenfunctions in Eqs. (15) and (16) which together form an orthonormal basis of $L^2(\Omega)$ at each time $t \in [0, T]$. Consider the finite set of the first M eigenfunctions $\phi_{mn}(r, z, t)$ with $m, n = 1, \ldots, M$, and note that by using the weight function $w(z, t) = \exp(-(\nu(t)/\kappa_0)z)$, then $\langle w(z, t)\phi_{mn}(r, z, t), \phi_{ps}(r, z, t)\rangle = \delta_{mp}\delta_{ns}$. We assume a solution of the form:

$$x(r, z, t) = \sum_{m,n=1}^{M} a_{mn}(t)\phi_{mn}(r, z, t) \tag{32}$$

where the coefficients $a_{mn}(t)$ are to be determined. Restricting $x(r, z, t)$ to the finite-dimensional space X which is spanned by $\phi_{mn}(r, z, t)$, then for each $t \in [0, T]$:

$$\int_{\Omega} w(z, t)\phi_{mn}(r, z, t)x(r, z, t)drdz = \sum_{p,s=0}^{M} a_{ps}(t)\int_{\Omega} w(z, t)\phi_{ps}(r, z, t)\phi_{mn}(r, z, t)drdz = a_{mn}(t)\delta_{mp}\delta_{ns} \tag{33}$$

with the indices $p, s = 1, \ldots, M$. The initial state is given by $a_{mn}(0) = \int_{\Omega}\phi_{mn}(r, z, t)x_0(r, z)drdz$ and the projection of Eq. (26) on X yields the system of M ordinary differential equations:

$$\frac{da_{mn}}{dt} = \Lambda_{mn}(t)a_{mn} + b_{mn}(t)u(t) \tag{34}$$

where

$$b_{mn}(t) = \int_{\Omega} b(z_c)w(z, t)\phi_{mn}(1, z, t)\phi_{mn}(r, z, t)drdz \tag{35}$$

The problem of determining a sufficiently large M such that the dominant dynamics of the PDE system may be captured in a finite set of M modes is considered in several other works (see for example [4,15]).

5.2. Optimal control problem for coupled systems

As previously stated, the crystal temperature dynamics are coupled to the domain motion through the boundary evolution at $z = l(t)$ and the boundary velocity $v(t)$ which are determined by the mechanical pulling arm and correspond to the states $q_1(t)$ and $q_2(t)$ in Eq. (36), respectively. The coupling of the infinite-dimensional system and the finite-dimensional subsystem is unidirectional since the crystal temperature does not affect the boundary motion. Therefore, one can consider the simultaneous stabilization of the domain motion and the crystal temperature regulation in the following setup.

The finite-dimensional state system representation of Eq. (1) which is used to model the pulling arm subsystem dynamics is given by:

$$\begin{pmatrix}\dot{q}_1\\ \dot{q}_2\end{pmatrix} = \begin{pmatrix}0 & 1\\ -b_e/m_s & -a_d/m_s\end{pmatrix}\begin{pmatrix}q_1\\ q_2\end{pmatrix} + \begin{pmatrix}0\\ 1/m_s\end{pmatrix}f_{\text{mec}} \tag{36}$$

where $q_1(t) = \tilde{l}(t)$ and $q_2(t) = \dot{\tilde{l}}(t) = v(t)$ are the states of the system denoted as:

$$\dot{q} = A_m q + B_m f_{\text{mec}} \tag{37}$$

The optimal control input for each of the systems is then simultaneously determined by augmenting Eq. (34) with Eq. (37) in the following setup:

$$\begin{pmatrix}\dot{q}\\ \dot{a}\end{pmatrix} = \begin{pmatrix}A_m & 0\\ 0 & \Lambda(t)\end{pmatrix}\begin{pmatrix}q\\ a\end{pmatrix} + \begin{pmatrix}B_m & 0\\ 0 & b\end{pmatrix}\begin{pmatrix}f_{\text{mec}}\\ u\end{pmatrix} \tag{38}$$

which is represented by $\dot{x}(t) = A_c(t)x(t) + B_c(t)F(t)$. The feedback control law for the augmented system in Eq. (38) is given by:

$$F_{\text{opt}}(t) = -R_c^{-1}B_c^{T}\Pi_c\boldsymbol{x} = \begin{pmatrix}f_{\text{opt}}(t)\\ u_{\text{opt}}(t)\end{pmatrix} \tag{39}$$

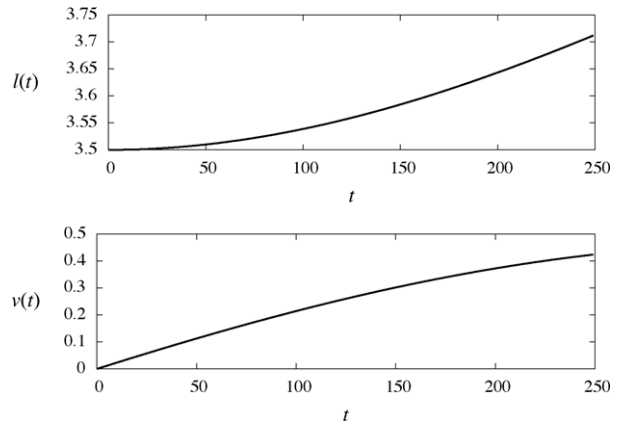

Fig. 2. Domain length and boundary velocity evolution. Dimensionless system parameters: $m_s = 0.75$, $a_e = 1$, $b_d = -2.5$. Control parameters: $Q_m = 0.5I_{2\times 2}$, $R_m = 1.5$.

where Π_c is determined from the solution of the augmented finite-dimensional differential Riccati equation analogous to Eq. (29).

6. Simulation results

In this section, the numerical simulation of the crystal temperature regulation problem in the presence of the time-varying spatial domain is provided. We consider the situation in which a perturbation has occurred in the crystal temperature distribution which arises, for example, from fluctuations in the melt environment. It is of interest to optimally stabilize the crystal temperature around the nominal steady state distribution of $x(r, z, t) = 0$ throughout the crystal region which is approximated as an axisymmetric cylinder with radius $R = 1$ and initial length $l(t = 0) = 3.5$ where the moving boundary at $z = l(t)$ and boundary velocity of $v(t)$ which are determined by the mechanical pulling arm at $z = 0$ drawing the crystal from the melt. To demonstrate the regulation of the crystal temperature in the presence of the time-varying spatial domain, the controller for the mechanical pulling arm subsystem is applied such that the domain growth is non-constant throughout the simulation and this point is further discussed in the following section.

6.1. Crystal temperature regulation

To capture the dominant dynamics of the crystal temperature evolution, the number of modes utilized was $M = 10$ for the finite-dimensional system representation of the PDE as described in the Section 5.1 with spatial discretization $\Delta r = 0.01$ for $[0 \le r \le 1]$ and $\Delta z = 0.025$ for $[0 \le z \le 3.5]$. The total simulation time of 250 time units t is representative of a physical processing time of 8 min, or 1.92 s per time unit.

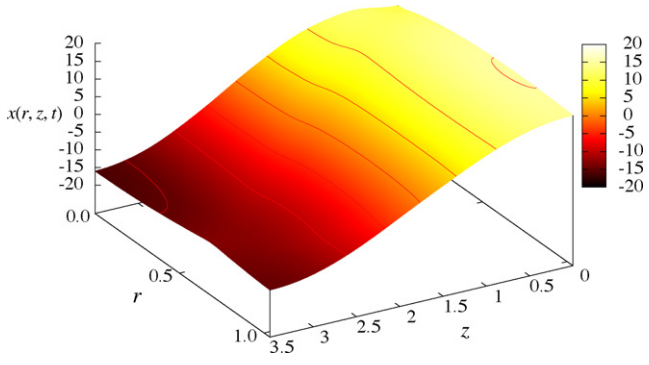

Fig. 3. Initial deviation form for the temperature distribution of crystal at $t = 0$. Crystal conductivity ratio $\kappa_0 = 0.39$.

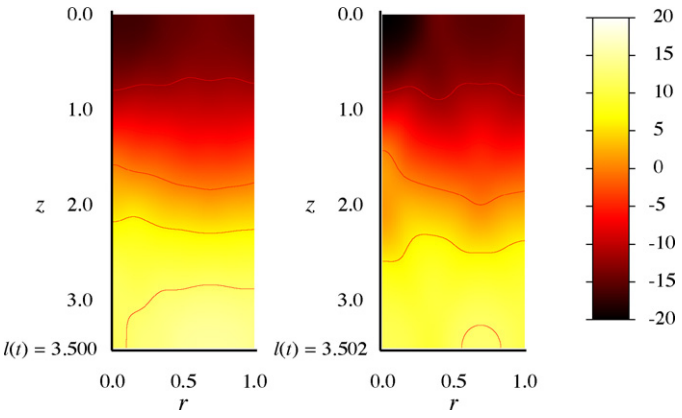

Fig. 4. Crystal temperature distribution at $t = 5$ (Left) and at $t = 25$ (Right).

The domain length and boundary velocity evolution are shown in Fig. 2. The total change in crystal length from $t = 0$ to $t = 250$ is approximately 0.21 units of length which corresponds to a physical system growth of 0.67 cm based on an average crystal pull rate of 5.0 cm/h [9]. From a practical point of view, the slow growth of the crystal is essential in preventing the occurrence of "necking" which results in crystals of non-uniform diameter. Aggressive control action on the crystal pull rate may also lead to undesirable instabilities in the meniscus shape whereby the melt separates from the solidified crystal (see [6]). The initial deviation form for the temperature distribution of the crystal is shown in Fig. 3 where the region on the side of the crystal–melt interface at $z = 3.5$ is higher than on the side of the pulling arm at $z = 0$. The optimal control law in Eq. (39) was numerically determined utilizing the first three modes of the finite-dimensional system representation of the PDE, with control parameters $Q(1, 1) = 10$, $Q(2, 2) = 1$, $Q(3, 3) = 0.0001$ and $\mathcal{R} = 0.005$. This was done to yield a low dimensional controller and also to prevent the peaking phenomena in the controller input to the system (see [24]). The optimal feedback control u_{opt} is calculated by solving the analogous finite-dimensional form of the time-varying differential Riccati equation in Eq. (29) at each time instance. The resulting input is applied at the $r = 1$ boundary of the crystal in the region $[0.2 \le z_c \le l(t)]$ and the output is measured at $r = 1$ and $z_o = 2.5$. Figs. 4–6 show the closed loop system temperature distribution $x(r, z, t)$ of the crystal at six different time instances: $t = 5, 25, 50, 75, 100, 150$ under the optimal control regulator. One can notice the temperature on the side of the crystal–melt interface at $z = l(t)$ is higher than on the side of the pulling arm at $z = 0$. At $t = 5$, the temperature difference between the highest and lowest

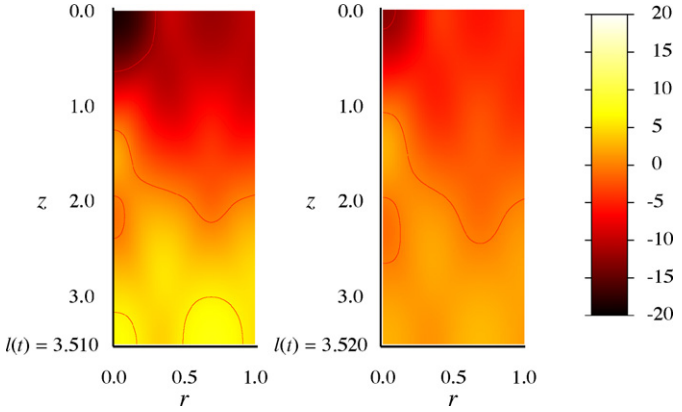

Fig. 5. Crystal temperature distribution at $t = 50$ (Left) and at $t = 75$ (Right).

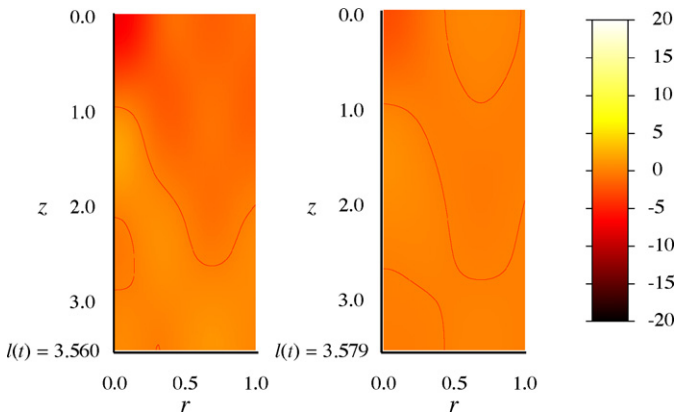

Fig. 6. Crystal temperature distribution at $t = 100$ (Left) and at $t = 150$ (Right).

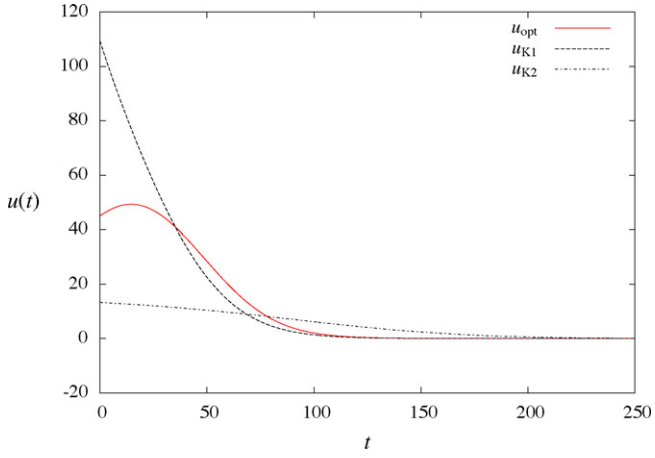

Fig. 7. Input profiles $u_{K1}(t)$, $u_{K2}(t)$, and $u_{\text{opt}}(t)$ applied to boundary of the crystal.

regions within the crystal is approximately 40 with the contours providing an indication of the overall temperature gradient across the crystal regions throughout the process. The temperature distribution becomes progressively uniform and stabilizes around the nominal distribution $x(r, z, t) = 0$ throughout almost the entire time-dependent region with crystal length $l(t) = 3.579$ at the time $t = 150$. The input profile generated by the optimal control scheme and the

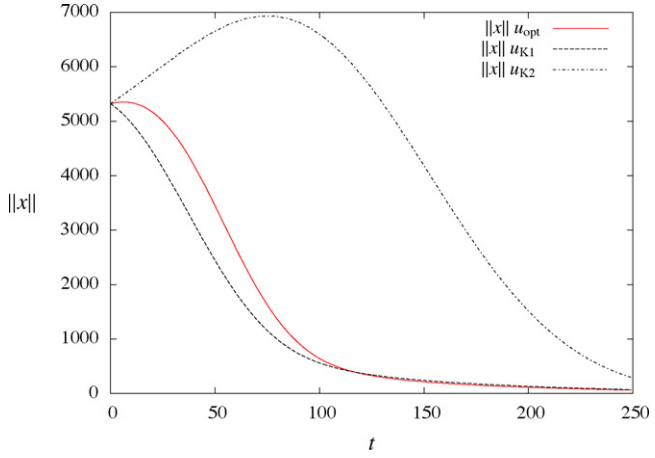

Fig. 8. Total system energy profiles for closed loop systems under $u_{K1}(t)$, $u_{K2}(t)$, and $u_{\text{opt}}(t)$.

total system energy evolution are shown in the following section with comparisons to simpler control strategies, see Figs. 7 and 8.

6.2. Comparison to fixed-gain controllers

To evaluate the performance of the optimal controller for the crystal temperature regulation problem, we consider the input and total energy profiles of the closed loop system as compared with two fixed-gain controllers. In contrast to the optimal controller, with time-varying gain $K_{\text{opt}}(t)$ which is determined from the solution of the differential Riccati equation, the two low dimensional modal based proportional controllers for the PDE system with time-invariant gains are selected as: $K_1 = (8; -1; -10)$; and $K_2 = (1; -0.5; -1)$. Each of K_1 and K_2 results in a control input $u_{K1}(t)$ and $u_{K2}(t)$. Each of the fixed-gain controllers, where the rate of temperature regulation is fixed such that the input evolution cannot be adjusted during the process, is not optimal, i.e. the gains are not chosen from any model based control criteria to incorporate any performance characteristics. The closed loop systems under each regulator with inputs $u_{K1}(t)$ and $u_{K2}(t)$ are simulated under the same conditions as the closed loop system under the optimal control law with input $u_{\text{opt}}(t)$.

Fig. 7 shows the input profiles $u_{K1}(t)$, $u_{K2}(t)$, and $u_{\text{opt}}(t)$. One can notice that the input generated using the fixed-gain controller K_1 resulted in a relatively more aggressive controller and highest initial input $u(t)$ as compared to each of $K_{\text{opt}}(t)$ and K_2. The least aggressive controller K_2 generated the input profile $u_{K2}(t)$. These results are consistent to what was expected due to the choice of entries in the gain vectors K_1 and K_2.

The total system energy profiles of the closed loop systems under each of the controllers $u_{K1}(t)$, $u_{K2}(t)$, and $u_{\text{opt}}(t)$ is shown in Fig. 8. It can be seen that aggressive controller resulted in the system initially being stabilized to a lower total energy than both of the controllers K_1 and $K_{\text{opt}}(t)$. The least aggressive controller K_2 resulted in a total system energy profile which initially increases even though the system is inherently dissipative. This phenomena is due to the growth in the crystal domain from the melt which contributes to the total system energy. In contrast, the optimal controller $K_{\text{opt}}(t)$, which accounts for the crystal domain evolution, is less aggressive than the controller K_1, and results in the input profile shown in Fig. 7. The total system energy profile for the optimal controller is initially greater than the profile generated by the aggressive controller K_1. At approximately $t = 100$ one can see that the two profiles are essentially identical while the states for both cases are stabilized to the zero distribution at approximately $t = 250$. One can notice that the optimal and time-varying control strategy with milder input profile resulted in the same temperature regulation performance over the simulation time-frame as the aggressive fixed-gain controller. These results suggests that the optimal control law would be better suited as a temperature regulator where it is undesirable to subject the crystal boundary to high temperature inputs.

7. Summary

In this work, we considered the optimal control of the CZ crystal growth and temperature regulation problem. The convection–diffusion parabolic PDE process model of the crystal temperature dynamics defined on the time-varying spatial domain was derived from first principles continuum mechanics. The domain evolution was described by a second order ODE model for the mechanical pulling arm subsystem which is unidirectionally coupled to the crystal temperature dynamics. The representation of the parabolic PDE as a nonautonomous operator on an infinite-dimensional space was developed and the analytic expression and

properties of the associated two-parameter semigroup were presented. The optimal control problem for the time-varying system was provided in terms of the two-parameter semigroup based on the LQR formulation for infinite-dimensional time-varying systems theory. A numerical scheme was provided to facilitate the realization of the control problem by approximation of the PDEs as finite-dimensional system. The optimal control problem setup for the finite-dimensional representation of the PDE augmented with the finite-dimensional subsystem for the mechanical pulling are was presented. The numerical simulation of the CZ crystal growth process demonstrated the regulation of the crystal temperature using the optimal control formulation developed in this work. A comparison of the optimal and time-varying regulator performance to simple fixed-gain controllers showed the advantages of the optimal control strategy.

Appendix A. Formulation of the PDE model

The parabolic PDE of a material domain with moving boundary can be derived directly from first-principles continuum mechanics (see for example [17,18]) and yields a convection–diffusion model which is consistent with the governing equations of heat transfer which are utilized in previous works to describe the CZ crystal temperature dynamics (see [8]).

Let the simple body $\Omega \subset \mathbb{R}^3$ with material points, $\zeta = (\zeta_1, \zeta_2, \zeta_3) \in \Omega$, volume element dV and smooth boundary $\partial\Omega$, denote the crystal body with spatial points $\xi = (\xi_1, \xi_2, \xi_3) \in \mathbb{R}^3$ and volume element dv. Let Ω_0 be the initial configuration and $\Omega_t \subset \mathbb{R}^3$ be the configuration at time $t \in [0, T]$. The regular motion of Ω is determined by the C^1 mapping $\varphi_t : \Omega \to \mathbb{R}^3$ such that $\xi = \varphi_t(\zeta)$ and $\Omega_t = \varphi_t(\Omega)$, with C^1 inverse, $\varphi_t^{-1} : \varphi_t(\Omega_t) \to \Omega$. The material velocity of the motion $\boldsymbol{V : \Omega \times [0, T] \to R^3}$ is defined by

$$\boldsymbol{V}(\zeta, t) = \boldsymbol{V}_t(\zeta) = \frac{\partial \varphi}{\partial t}(\zeta, t) = \frac{d}{dt}\varphi_\zeta(t) \tag{A.1}$$

The spatial velocity of motion $\boldsymbol{\nu : \varphi_t(\Omega) \to R^3}$ defines the spatial velocity field ν with relation $\boldsymbol{\nu = V_t \circ \varphi_t^{-1}}$ where $\circ$ is the composition operator. The regularity of the motion presumes that Ω is never divided or penetrated and the continuous mapping φ_t allows one to describe the configuration of Ω at time $t \in [0, T]$ in terms of a fixed configuration by change of variables (see [17]).

We define the following standard identities: the Jacobian of $\varphi_t(\zeta)$ is $J(\zeta, t) = \det(\partial\varphi/\partial\zeta)$ with derivative $\partial J/\partial t = \nabla \cdot \boldsymbol{\nu} J(\zeta, t)$. Under the assumption that mass is conserved, one obtains that $(D\rho/Dt) + \rho\nabla \cdot \boldsymbol{\nu} = 0$, where $(D/Dt) = (\partial/\partial t) + \boldsymbol{\nu} \cdot \nabla$ is the material derivative operator.

The Transport Theorem which describes the rate of change of the crystal temperature x in Ω_t with respect to time is:

$$\begin{aligned}\frac{d}{dt}\int_{\varphi_t(\Omega)} \rho(\xi, t)x(\xi, t)dv &= \frac{d}{dt}\int_\Omega \rho(\varphi_t, t)x(\varphi_t, t)J(\zeta, t)\,dV \\ &= \int_\Omega \left(\frac{D\rho}{Dt}(\varphi_t, t)x(\varphi_t, t)J(\zeta, t) \right. \\ &+ \rho(\varphi_t, t)\frac{Dx}{Dt}(\varphi_t, t)J(\zeta, t) + \rho(\varphi_t, t)x \\ &\left. \times (\varphi_t, t)\frac{\partial J}{\partial t}(\zeta, t) \right) dV \end{aligned} \tag{A.2}$$

Using the identities and change of variables such that the differentiation and integration operations may be interchanged [18], we have:

$$\begin{aligned}\frac{d}{dt}\int_{\varphi_t(\Omega)} \rho(\xi, t)x(\xi, t)dv &= \int_\Omega \rho(\varphi_t, t)(-x(\varphi_t, t)\nabla \cdot \boldsymbol{\nu}(\varphi_t, t) \\ &+ \frac{\partial x}{\partial t} + \boldsymbol{\nu}(\varphi_t, t) \cdot \nabla x(\varphi_t, t)\,. \\ &+ x(\varphi_t, t)\nabla \cdot \boldsymbol{\nu}(\varphi_t, t))J(\zeta, t)dV \\ &= \int_\Omega \rho(\varphi_t, t)(\frac{\partial x}{\partial t}(\varphi_t, t) + \boldsymbol{\nu}(\varphi_t, t) \cdot \\ &\times \nabla x(\varphi_t, t))J(\zeta, t)\,dV \\ &= \int_{\varphi_t(\Omega)} \rho(\xi, t)\left(\frac{\partial x}{\partial t}(\xi, t) + \boldsymbol{\nu}(\xi, t) \cdot \right. \\ &\left. \times \nabla x(\xi, t) \right) dv \end{aligned} \tag{A.3}$$

Then by the Conservation Law the total heat balance in the region is expressed as $(d/dt) \int_{\Omega_t} \rho x dv = \int_{\partial\Omega_t} \kappa \nabla x \cdot n\, ds$, where κ is the thermal conductivity constant, and n is the normal component of ds. Substitution of Eq. (A.3) yields the expression:

$$\int_{\Omega_t} \rho(\xi, t)\left(\frac{\partial x}{\partial t}(\xi, t) + \boldsymbol{\nu}(\xi, t) \cdot \nabla x(\xi, t) \right) dv = \int_{\Omega_t} \nabla \cdot \kappa \nabla x(\xi, t) dv \tag{A.4}$$

From a physical point of view of the CZ crystal growth process, the following assumptions are made: the density of the solidified material at the crystal–melt interface is equal to that of the preexisting crystal such that $\rho(\xi, t) = \rho$ is constant. Secondly, the material growth is due to the motion of the boundary at the crystal–melt interface whereby $\boldsymbol{\nu(\xi, t) = \nu(t)}$. Furthermore, one can regard the element dv as the crystal regions itself which yields the differential form of Eq. (A.4):

$$\rho\left(\frac{\partial x}{\partial t} + \nu(t) \cdot \nabla x \right) = \nabla \cdot \kappa \nabla x \tag{A.5}$$

whereby Eq. (A.5) is the PDE which descirbes the temperature dynamics in the time-dependent spatial domain Ω_t where the domain deformation is due to the motion of the boundary with velocity $\nu(t)$. The scaling of Eq. (A.5) by the constant Peclet number, Pe, converts the PDE to the dimensional form in Eq. (2) which describes the CZ crystal temperature dynamics (see also [9,10]).

The temperature field across the crystal boundary in the axisymmetric radial direction and at the side of the pulling arm is assumed to be zero-flux [10]. The melt temperature x_m is assumed to be a constant C and equal to the crystal temperature at the melt–crystal interface boundary, i.e. $x_m = x(r, l(t), t) = C$ at $z = l(t)$ such that $\partial x/\partial z = 0$ at $z = l(t)$. Then the boundary conditions imposed on the PDE are prescribed as in Eq. (3).

Appendix B. Properties of $U(t, s)$

The property G1 is determined from the relation $\|U(t, s)\| \leq \exp\left\{ \int_s^t \|\mathcal{A}(\tau)\| d\tau \right\}$ which follows from the Contraction mapping principle where $z(t)$ is a fixed point associated with the homogeneous form of the initial value problem (see [19]). By Gronwall's inequality $\|U(t, s)z_0\| = \|z(t)\| \leq \|z_0\| \exp\left(\int_s^t \|\mathcal{A}(\tau)\| d\tau \right)$ whereby $U(t, s)$ is bounded, see [21].

The property G2 is determined as follows: consider the family of eigenfunctions in Eqs. (15) and (16) with indices m, m', n, $n' = 1, 2, \ldots$ and let $h_{mn}(t,s) = \lambda_n(t)t - \lambda_n(s)s - \kappa_0\alpha_m^2(t-s)$. One can note that the sets $\{\phi_{mn}(t)\}_{t\in[0,T]}$ and $\{\psi_{m'n'}(t)\}_{t\in[0,T]}$ are pairwise orthonormal for each $t \in [0, T]$:

$$\int_\Omega \phi_{mn}(r,z,t)\psi_{m'n'}(r,z,t)drd\xi = \begin{cases} 1, & m = m' \text{ and } n = n' \\ 0, & \text{otherwise} \end{cases} \quad \text{(B.1)}$$

The identity $U(t,t) = I$ is easily deduced by inspection. It follows that for $x \in L^2(\Omega)$ and $0 \le s \le s^* \le t \le T$:

$$U(t,s^*)U(s^*,s)x = \sum_{m,n=1}^{\infty} e^{h_{mn}(t,s^*)} \langle \sum_{p,q=1}^{\infty} e^{h_{pq}(s^*,s)} \langle x, \psi_{pq}(s)\rangle \phi_{pq}(s^*),$$

$$\psi_{mn}(s^*)\rangle\phi_{mn}(t) = \sum_{m,n=1}^{\infty} e^{h_{mn}(t,s)} \langle x, \psi_{mn}(s)\rangle\phi_{mn}(t)$$

$$= U(t,s)x$$

The property G3 is verified by direct calculation with:

$$\mathcal{A}(t)U(t,s) = \sum_{m,n=1}^{\infty} \mathcal{F}_{mn}(t) \left\langle \sum_{p,q=1}^{\infty} e^{h_{pq}(t,s)} < ., \psi_{pq}(s) > \phi_{pq}(t), \right.$$

$$\left. \psi_{mn}(t) \right\rangle \phi_{mn}(t) = \sum_{m,n=1}^{\infty} \mathcal{F}_{mn}(t) e^{h_{mn}(t)} < ., \psi_{mn}(s) > \phi_{mn}(t) \quad \text{(B.2)}$$

The operator $U(t,s)$ is differentiable in $t \in [0, T]$ and straightforward calculations yields:

$$\frac{\partial U(t,s)}{\partial t} = \sum_{m,n=1}^{\infty} \left\{ \left(t\frac{d}{dt}\lambda_n(t) + \lambda_n(t) - \kappa_0\alpha_m^2 \right) \phi_n^{(2)}(t) \right.$$

$$\left. + \frac{\partial \phi_n^{(2)}(t)}{\partial t} \right\} e^{h_{mn}(t,s)} \langle \cdot, \psi_n(s)\rangle \phi_m^{(1)} = \mathcal{A}(t)U(t,s) \quad \text{(B.3)}$$

The derivative of $U(t,s)$ with respect to $s \in [0, T]$ is similarly determined.

References

[1] P. Acquistapace, F. Flandoli, B. Terreni, Initial boundary value problems and optimal control for nonautonomous parabolic systems, SIAM J. Math. Anal. 29 (1991) 89–118.

[2] P. Acquistapace, B. Terreni, Infinite-horizon linear-quadratic regulator problems for nonautonomous parabolic systems with boundary control, SIAM J. Math. Anal. 34 (1996) 1–30.

[3] A. Armaou, P.D. Christofides, Robust control of parabolic PDE systems with time-dependent spatial domains, Automatica (2001).

[4] M. Balas, Exponentially stabilizing finite-dimensional controllers for linear distributed parameter systems: Galerkin approximation of infinite-dimensional controllers, J. Math. Anal. Appl. 117 (1986) 358–384.

[5] A. Bensoussan, G.D. Prato, M. Delfour, S. Mitter, in: Representation and Control of Infinite Dimensional Systems, Birkhäser, Boston, 2007.

[6] R. Brown, Theory of transport processes in single crystal growth from the melt, AIChE J. 34 (1988) 881–911.

[7] J. Derby, R. Brown, Thermal-capillary analysis of czochralski and liquid encapsulated czochralski crystal growth: I. Simulation, J. Cryst. Growth 74 (1986) 605–624.

[8] J. Derby, R. Brown, Thermal-capillary analysis of czochralski and liquid encapsulated czochralski crystal growth: II. Processing strategies, J. Cryst. Growth 75 (1986) 227–240.

[9] J. Derby, R. Brown, On the dynamics of czochralski crystal growth, J. Cryst. Growth 83 (1987) 137–151.

[10] J.J. Derby, L.J. Atherton, P.D. Thomas, R.A. Brown, Finite-element methods for analysis of the dynamics and control of czochralski crystal growth, J. Sci. Comput. 2 (1987) 297–343.

[11] W. Dunbar, N. Petit, P. Rouchon, P. Martin, Boundary control of a nonlinear stefan problem., in: Decision and Control, 2003. Proceedings. 42nd IEEE Conference on. vol. 2, 2003, pp. 1309–1314.

[12] L. Evans, in: Partial Differential Equations, Amer. Mathematical Society, USA, 1998.

[13] M. Hinze, S. Ziegenbalg, Optimal control of the free boundary in a two-phase stefan problem, J. Comput. Phys. 223 (2) (2007) 657–684.

[14] T. Hughes, in: The Finite Element Method, Dover Publications, New York, USA, 2000.

[15] K. Ito, Finite-dimensional compensators for infinite-dimensional systems via galerkin-type approximation, SIAM J. Control Optim. 28 (1990) 1251–1269.

[16] C.W. Lan, Recent progress of crystal growth modeling and growth control, Chem. Eng. Sci. 59 (7) (2004) 1437–1457.

[17] J. Marsden, T. Hughes, in: Mathematical Foundations of Elasticity, Dover Publications, New York, USA, 1983.

[18] J. Marsden, T. Ratiu, R. Abraham, in: Manifolds, Tensor Analysis and Applications, Springer-Verlag, New York, USA, 2001.

[19] R. McOwen, in: Partial Differential Equations: Methods and Applications, 2nd ed., Prentice Hall, USA, 2002.

[20] D. Naidu, in: Optimal Control Systems. Electrical Engineering Textbook Series, CRC Press, 2003.

[21] A. Pazy, in: Semigroups of Linear Operators and Applications to Partial Differential Equations, Springer-Verlag, New York, USA, 1983.

[22] W. Ray, in: Advanced Process Control, McGraw-Hill, New York, 1981.

[23] T. Sinno, R.A. Brown, Modeling microdefect formation in czochralski silicon, J. Electrochem. Soc. 146 (6) (1999) 2300–2312.

[24] H.J. Sussmann, P.V. Kokotovic, The peaking phenomenon and the global stabilization of nonlinear systems, IEEE Trans. Automat. Contr. 36 (1991) 424–440.

[25] G. Szabo, Thermal strain during czochralski crystal growth, J. Cryst. Growth 73 (1985) 131–141.

[26] P.K.C. Wang, Stabilization and control of distributed systems with time-dependent spatial domains, J. Optim. Theor. Appl. 65 (1990) 331–362.

[27] P.K.C. Wang, Feedback control of a heat diffusion system with time-dependent spatial domains, Optim. Contr. Appl. Meth. 16 (1995) 305–320.